European Review for Medical and Pharmacological Sciences 2019; 23: 1279-1290

Cellular mechanism of Tβ4 intervention in liver fibrosis by regulating NF-κB signaling pathway

Z.-X. ZHU[1,2], L.-L. ZHU[3], Z. CHENG[4], X.-K. ZHAO[2], Y.-M. LIU[2], L.-D. FAN[1,2], G.-L. ZOU[1,2], Q.-Y. OUYANG[1,2], M.-L. CHENG[2]

[1]Department of Clinical Medicine, Guizhou Medical University, Guiyang, P. R. China.
[2]Department of Infectious Diseases, The Affiliated Hospital of Guizhou Medical University, Guiyang, P. R. China.
[3]Department of Blood Transfusion, The Affiliated Hospital of Guizhou Medical University, Guiyang, P. R. China.
[4]School of Basic Medical Sciences, Peking University Health Science Center, Beijing, P. R. China.

Abstract. – OBJECTIVE: To investigate the inhibitory effect of thymosin-β4 (Tβ4) on the activation of the human hepatic stellate cell line (HSC-LX2) induced by interleukin (IL)-1β.

MATERIALS AND METHODS: There were 5 groups in this study, i.e., blank control group, negative control group (SI-NC, empty plasmid), model group (20 ng/ml of IL-1β), siRNA-Tβ4 knockdown group (IL-1β and si-Tβ4) and Tβ4 treatment group (IL-1β and 1000 ng/ml of Tβ4). Cell proliferation rate was measured using the Cell Counting Kit-8 (CCK-8) method. The cell cycle change and percentage of apoptotic cells were determined by Propidium Iodide (PI) DNA staining and Annexin V-fluorescein isothiocyanate (FITC) double staining. Cellular nucleic acid levels of p-IKB and nuclear factor-kappa B (NF-κB)/p65 proteins were measured by fluorescent quantitative Real Time-Polymerase Chain Reaction (RT-PCR). Double immunofluorescence staining and Western blot were used to detect nuclear translocation of NF-κB and p65 and levels of cytoplasmic p-IKB protein and nuclear p65 protein.

RESULTS: Due to the G0/G1 phase arrest, the number of cells in the Tβ4 treatment group increased, compared with the model group and the siRNA-Tβ4 knockdown group ($p<0.01$). In the same between-group comparison, apoptotic rate in the Tβ4 treatment group increased significantly ($p<0.05$). The cellular nucleic acid levels of p-IKB and NF-κB/p65 were markedly higher in the model group and the siRNA-Tβ4 knockdown group than in the blank control group ($p<0.01$). The cellular nucleic acid levels of p-IKB and NF-κB/p65 were remarkably lower in the Tβ4 treatment group than in the siRNA-Tβ4 knockdown group ($p<0.01$). The expression levels of NF-κB/p65 and NF-κB/p50 were significantly lower in the Tβ4 treatment group. The expression levels of cytoplasmic p-IKB and nuclear NF-κB/p65 were lower in the Tβ4 treatment group than in the model group ($p<0.01$).

CONCLUSIONS: Tβ4 significantly inhibited IL-1β-induced HSC-LX2 cell proliferation. The mechanism may involve decreased activation of the NF-κB pathway, decreased expression of p-IKB and nuclear translocation of p65. Therefore, Tβ4 had the effect of reversing liver fibrosis.

Key Words
Liver fibrosis, Thymosin-β4, NF-κB signaling pathway, IL-1β.

Introduction

Thymosin-β4 (Tβ4) is a leading regulatory factor of actin, which participates in various biological processes in human body. It is closely associated with tissue regeneration, wound healing, apoptosis, inflammatory response, angiogenesis, and the onset and metastasis of some cancers[1,2]. In animal models of endotoxin-induced septic shock, Tβ4 can reduce the mortality rate by inhibiting the release of large amounts of inflammatory mediators and decreasing the infiltration of inflammatory cells[3,4].

Liver fibrosis refers to abnormal proliferation and accumulation of connective tissue in the liver caused by various pathogenic factors. Clinically, it is a chronic disease manifesting with diffuse and excessive deposition of extracellular matrix in the liver[5-7]. The activation of hepatic stellate cells is a core event of liver fibrosis, which leads to increased cell proliferation and increased collagen synthesis. Meanwhile, the cells acquire contractility, further promoting the onset and progression of liver fibrosis. The activation of nuclear factor-kappa B (NF-κB) is observed in almost all inflammatory

Corresponding Author: Mingliang Cheng, MD; e-mail: mcw23b@163.com

cells. Hepatic stellate cell (HSC) activation is associated with secretion of various inflammatory mediators regulated by the NF-κB signaling pathway. NF-κB exists primarily as a heterodimer of p50 and p65 subunits. The NF-κB pathway is activated through IκBα ubiquitination and degradation after binding to the p65 subunit. NF-κB activation was followed by nuclear translocation and transcriptional expression of target genes[8-10]. According to Zhu et al[11], Tβ4 exhibited anti-fibrotic effect by regulating the PI3K/AKT/mTOR pathway in HSC. As a PI3K-related signal pathway, it is not fully understood if the NF-κB signaling pathway is associated with Tβ4's anti-fibrotic effect. Therefore, in this work, we investigated whether Tβ4 can promote the apoptosis of HSC and reverse liver fibrosis by regulating the PI3K-related NF-κB pathway.

Materials and Methods

Cell Line Used in This Study

The rat hepatic stellate cell line HSC-LX2 was purchased from the Institute of Biochemistry and Cell Biology affiliated with the Shanghai Institute of Biological Sciences and Chinese Academy of Sciences.

CCK8 Method Assessing Cell Proliferation

LX2 cells in good growth state were seeded into a 96-well culture plate at a density of 1×10^5 cells/mL after digestion. The cells were divided into normal control group and Tβ4 treatment group, and were synchronized after culturing for 24 h. After synchronization, Tβ4 at different concentrations (0.1, 1, 10, 100, 1000 ng/mL) was sequentially added to cells in the Tβ4 treatment group. After 24 h incubation, the medium in each well was aspirated, followed by addition of serum-free high glucose Dulbecco's Modified Eagle Medium (DMEM; Gibco, Grand Island, NY, USA; 100 μL/well) and Cell Counting Kit-8 (CCK-8; Dojindo, Kumamoto, Japan; 20 μL/well). After incubation for 4 h, the supernatant was discarded. The absorbance value (A) of each well was measured at 450 nm by a microplate reader. The cell growth inhibition rate was calculated using formula:

cell growth inhibition rate = $1 - [(OD_{treatment} - OD_{zeroing}) / (OD_{control} - OD_{zeroing})] \times 100\%$.

Cell Grouping Based on Cell Growth Inhibition Rates

According to appropriate drug use window, HSC-LX2 cells during the logarithmic phase of growth were divided into five groups: blank control group, negative control group (SI-NC, empty plasmid), model group (20 ng/mL of interleukin (IL)-1β), siRNA-Tβ4 knockdown group (IL-1β and si-Tβ4), and Tβ4 treatment group (IL-1β and 1000 ng/mL of Tβ4).

SiRNA Transfection of Tβ4 Site

The cDNA sequence of Tβ4 was looked up in the NCBI GenBank database. Tβ4 siRNA was synthesized following siRNA design principles. Primer synthesis and plasmid construction were completed by GenePharma (Shanghai, China). Before transfection, LX2 cells during the logarithmic phase were seeded into a 6-well plate at 4×10^5 cells/well. When cell fusion rate reached 40%, the supernatant was aspirated. The LX2 cells were transfected with plasmid vectors containing silent and nonsense mutations. After transfection for 24 h, the medium in each well was replaced with high glucose DMEM supplemented with 10% fetal bovine serum (FBS; Gibco, Grand Island, NY, USA). Puromycin (final concentration 5 μg/mL) was added to select stably expressing clones. The gradient screening took 4 d of incubation. Single cell clones showing green fluorescence were visualized under a fluorescence microscope. The positive clones were expanded in plates. In the end, stably transfected LX2 cell line was obtained. After screening, the nonsense cell clones with stable expression was assigned to the negative control group.

Cell Cycle Analysis by Propidium Iodide (PI)

Cells in each group were rinsed twice with pre-cooled Phosphate-Buffered Saline (PBS; Gibco, Grand Island, NY, USA). Following trypsin digestion, cells were blown gently with fresh medium. After centrifugation at 4°C and 1200 rpm for 5 min, the supernatant was discarded. The pellet was blown with 5 mL of pre-cooled ethanol. After sealed with a sealing film, the cells were fixed overnight at 4°C. Following fixation, the cells were re-suspended in 0.5 mL of PBS and transferred to a flow cytometry tube. In the flow tube, the final concentration was about 55 μg/mL by adding 3 μL of RNase-A solution. The final concentration of Propidium Iodide (PI) was about 65 μg/mL by adding about 50 μL of Propidium Iodide. The mixture was kept in the dark for 25 min. After filtration with 300-mesh nylon net, the sample was measured using a flow cytometer.

Detection of Apoptosis by Annexin V-FITC Double Staining

Cells in each group were re-suspended in 1× binding buffer, followed by adding 5 μL of Annexin V-fluorescein isothiocyanate (FITC; Beyotime, Shanghai, China) dye. The mixture was vortexed and incubated in the dark for 20 min. The incubation was continued in the dark for another 4-6 min after adding 10 μL of Propidium Iodide (PI) dye. Cells were re-suspended if necessary. After filtration with 300-mesh nylon net, the sample was measured using a flow cytometer.

Cellular Nucleic Acid Levels of p-IKB and NF-κB/p65 Proteins Measured by Fluorescent Quantitative Real Time-Polymerase Chain Reaction (RT-PCR)

After treatment, the cell suspension in each group was centrifuged. Total RNA was extracted and purified from the pellet by the TRIzol-phenol-chloroform one-step method. Its integrity, concentration and purity were analyzed. Complementary DNA (cDNA) was synthesized from the obtained RNA via reverse transcription according to the user manual of First Strand cDNA Synthesis Kit. Real Time-Polymerase Chain Reaction (RT-PCR) was then carried out to amplify the DNA sequence. In the experiment, β-actin was used as an internal reference gene, and the copy number (Ct value) of each sample was obtained after a standardized conversion. The analysis was performed by the $2^{-\Delta\Delta CT}$ method, and the result was obtained by calculation using the Ct value.

Nuclear Translocation of NF-κB/p65, NF-κB/p50 and p-IKB in HSC-LX2 Cells in Each Group Detected by Double Immunofluorescence Staining

Cells were cultured in a confocal dish. After treatment in each group, the cells were fixed using 4% formaldehyde at room temperature, followed by permeabilization with 0.2% Triton X-100 and blocked with 5% bovine serum Albumin (BSA). The primary antibody was added, and the cells were incubated at 4°C in a wet box overnight. The secondary antibody was then added, and the cells were incubated in the dark. The cells were further stained with dropwise added DAPI. Following staining, the cells were washed three times with PBS. An anti-fluorescence quenching solution was added dropwise to the cells, followed by mounting onto coverslips. The coverslips were observed under a confocal microscope in 3 fluorescence channels, and the images were combined.

Box. LX2 p-IκB, NF-κBp65 mRNA Primer.

Gene	^	Primer sequence
GAPHD	F	5'-GACCTGACCTGCCGTCTA-3'
	R	5'-ATCTGCCGTCCAGTCCAG-3'
IκB	F	5'-GAGTGCGTGCAGAAGTATCAA-3'
	R	5'-CCACAGAACAGCCAACCAG-3'
NF-κBp65	F	5'-GGGGACTACGACCTGAATG-3'
^	R	5'-GGGCACGATTGTCAAAGAT-3'

Western Blot Measurement of Cytoplasmic p-IKB Protein and Nuclear p65 Protein in IL-1β-Stimulated HSC-LX2 Cells After Tβ4 Treatment

Cell lysis buffer was added to the treated LX2 cells in each group, followed by incubation on ice for 20 min. Total protein was extracted after centrifugation, and the concentration was measured by the BCA method. A 12% polyacrylamide gel electrophoresis solution was freshly made. A sample of the total protein was loaded onto the 12% gel. After electrophoresis, the protein bands were transferred to nitrocellulose membrane. Non-specific binding sites in the membrane were blocked with PBS solution containing 5% skimmed milk powder. After washing the membrane, the specific primary antibody (1:1000 dilution) was added, followed by incubation at 4°C overnight on a rocking platform. Then, the horseradish peroxidase-labeled goat anti-rabbit IgG secondary antibody (1:4000 dilution) was added, followed by incubation for 2 hours and exposure with a chemiluminescent agent. The gray scale values of gel strips were analyzed by the gel imaging system. Semi-quantitative analysis was performed by the ratio of the integrated optical density of the target band and the internal reference β-actin band.

Statistical Analysis

All data were analyzed using the SPSS 19.0 statistical software (SPSS Inc., Chicago, IL, USA). The experimental data were expressed as mean ± standard deviation. The *t*-test was used in the pairwise comparison. One-way analysis of variance was used in comparison between multiple groups. The SNK-q test was used when the variances were equal, and the Tamhane's T2 test was used when the variances were not equal. The LSD method was used for pairwise comparison. A difference was statistically significant when $p<0.05$.

Table I. Toxicity of Tβ4 to HSC-LX2 cells.

Tβ4 concentration (ng/mL)	n	Absorbance	Inhibition rate (%)
0	3	4.4973±0.0379	0
1	3	3.6156±0.0208	18
10	3	2.9158±0.0515	35
100	3	2.6610±0.0676	40
1,000	3	2.3663± 0.0481	47
10,000	3	1.3903±0.0339	69
100,000	3	0.6802±0.0445	84

Results

Toxicity of Tβ4 for LX2 Cells

The results showed that Tβ4 can inhibit cell proliferation, and its IC50 for inhibiting LX2 cells for 24 h was 1248.6 ng/mL. The IC50 was obtained by calculation using the regression equation. In subsequent experiments, a drug concentration no greater than 1000 ng/mL was used. The toxicity results were shown in Table I.

Cell Transfection Observed Under a Fluorescence Microscope

Figure 1 showed cell transfection observed under a fluorescence microscope.

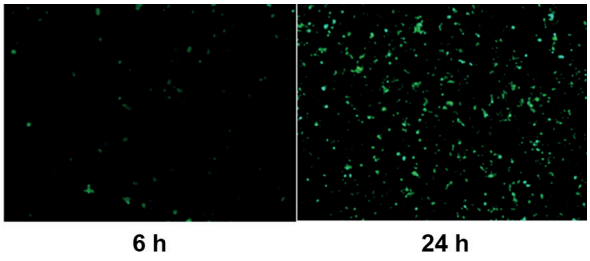

Figure 1. Representative image in the same field of view after cell transfection screening under fluorescence microscope (x100).

Alteration of LX2 Cell Cycle After Tβ4 Treatment Detected by Flow Cytometry

Compared with the model group and the siRNA-Tβ4 knockdown group, the number of cells in the Tβ4 treatment group increased due to the G0/G1 phase arrest ($p<0.01$), suggesting that inhibition of Tβ4 can interfere with cell cycle progression and hinder differentiation and maturation of the LX2 cells (See Table II and Figure 2).

Detection of Tβ4-Induced Apoptosis of LX2 Cells by Flow Cytometry

Late apoptotic cells were stained by both PI and Annexin V (PI+/AnnexinV+), as shown in the Q2 zone, whereas early apoptotic cells were stained by Annexin V but not PI (PI-/AnnexinV+), as shown in the Q3 zone. Compared with the model group and the siRNA-Tβ4 knockdown group, the apoptotic rate in the Tβ4 treatment group increased significantly, reaching 17%, and the differences were statistically significant ($p<0.05$). There was no significant difference in the apoptotic rate between the model group and the siRNA-Tβ4 knockdown group ($p>0.05$). These findings suggested that the knockdown of Tβ4 can hinder apoptosis of HSC-LX2 cells (See Table III and Figure 3).

Table II. Alteration of LX2 cell cycle after Tβ4 treatment detected by flow cytometry (x±s).

Group	n	G0G1 (%)	S	G2M
Blank control group	3	54.05±0.127	32.48±0.225	17.27±0.412
Negative control group	3	50.96±0.146	31.77±0.234	18.09±0.292
Model group	3	36.39±0.254**	33.91±0.315**	29.69±0.325**
siRNA-Tβ4 knockdown group	3	33.10±0.375**	41.71±0.412**	25.18±0.133*
Tβ4 treatment group	3	74.98±0.412**$^{\#\#}$	11.65±0.214*$^{\#\#}$	13.37±0.224$^{\#}$

*$p<0.05$, compared with the blank control group; **$p<0.01$, compared with the blank control group; $^{\#}p<0.05$, compared with siRNA-Tβ4 knockdown group; $^{\#\#}p<0.01$, compared with siRNA-Tβ4 knockdown group.

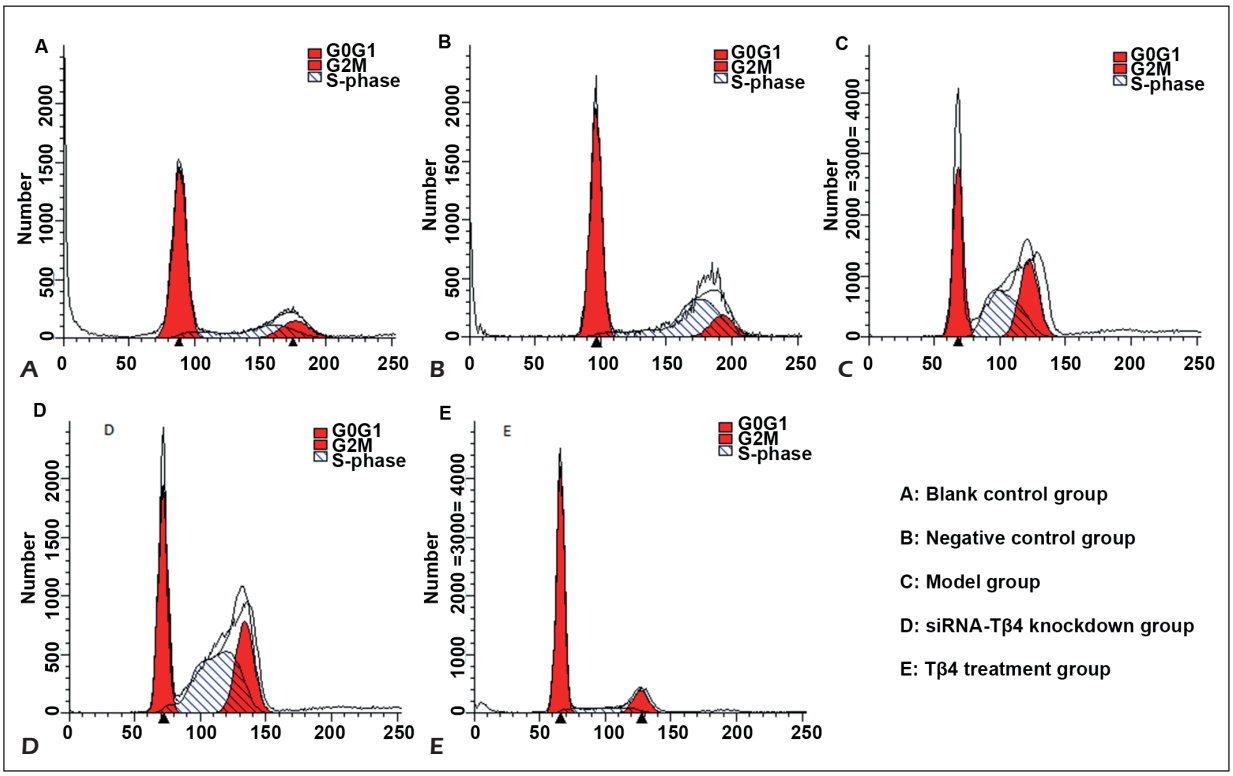

Figure 2. Alteration of LX2 cell cycle after Tβ4 treatment.

Measurement of Nucleic Acid Expression Levels of p-IKB and NF-κB/p65 by qRT-PCR

The cellular nucleic acid levels of p-IKB and NF-κB/p65 were significantly higher in the model group and the siRNA-Tβ4 knockdown group than in the blank control group (p<0.01). The cellular nucleic acid levels of p-IKB and NF-κB/p65 were markedly lower in the Tβ4 treatment group than in the siRNA-Tβ4 knockdown group (p<0.01). These findings suggested that Tβ4 knockdown can promote IKB phosphorylation in HSC-LX2 cells and increase mRNA expression of NF-κB/p65. The mRNA expression level of p-IKB in the siRNA-Tβ4 knockdown group was slightly higher than that in the model group, but there was no significant difference (p>0.05; see Table IV and Figure 4).

Table III. Detection of Tβ4-induced apoptosis of HSC-LX2 cells by flow cytometry (x±s).

Group	No	Apoptotic rate (%)
Blank control group	3	1.91±0.032#
Negative control group	3	1.82±0.021#
Model group	3	0.63±0.0646*
siRNA-Tβ4 knockdown group	3	0.73±0.145*
Tβ4 treatment group	3	17.12±0.456**

*p<0.05, compared with the blank control group; **p<0.01, compared with the blank control group; #p<0.05, compared with siRNA-Tβ4 knockdown group; ##p<0.01, compared with siRNA-Tβ4 knockdown group.

Nuclear Translocation of NF-κB/p65 and NF-κB/p50 in HSC-LX2 Cells Detected by Immunofluorescence Staining and Laser Confocal Microscopy

Very low expression levels of NF-κB/p65 and NF-κB/p50 in cell nuclei were observed in the control group, whereas in the model group and the siRNA-Tβ4 knockdown group the fluorescence intensity increased significantly, indicating higher levels of NF-κB/p65 and NF-κB/p50 in cell nuclei. The results demonstrated occurrence of nuclear translocation in activated HSC. In the Tβ4 treatment group, the fluorescence intensity decreased remarkably, indicating lower levels of NF-κB/p65 and NF-

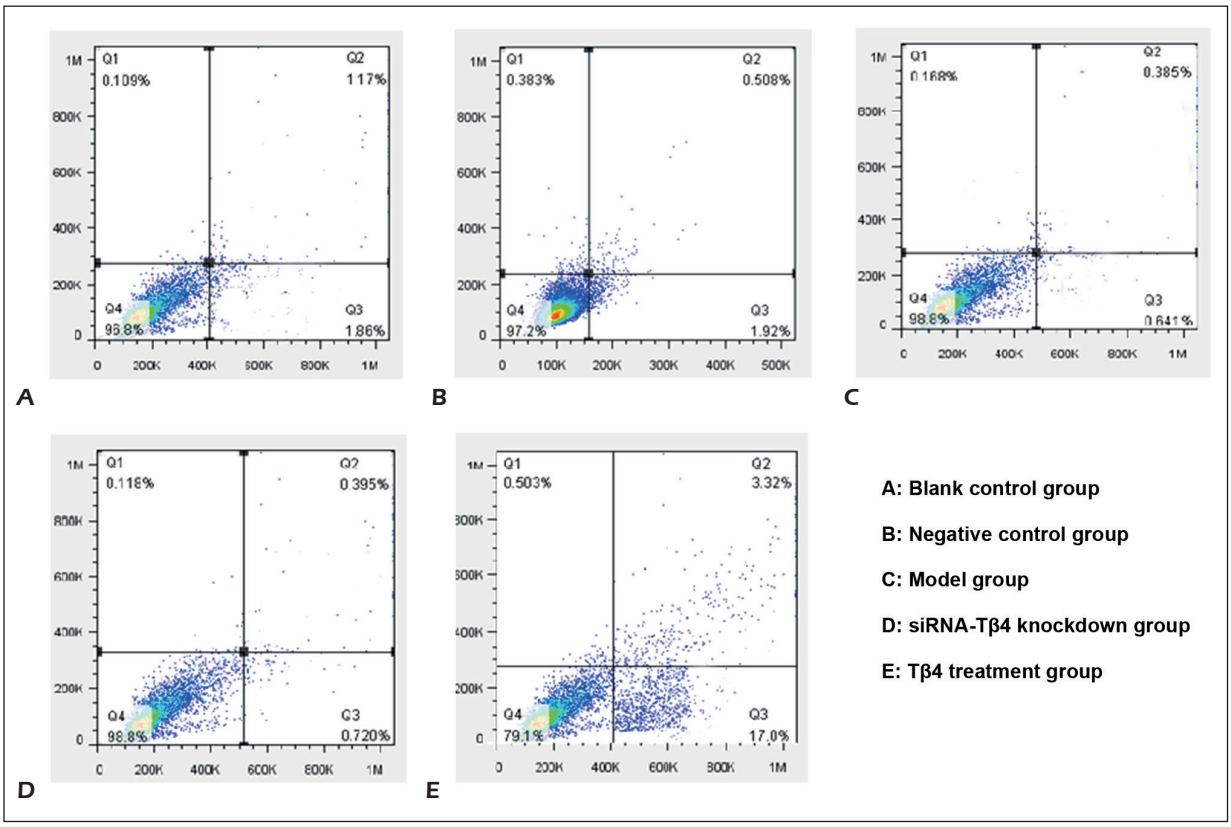

Figure 3. Detection of apoptosis of HSC-LX2 cells by Annexin V/PI double staining.

Table IV. Tβ4-induced alteration of mRNA expression levels of p-IKB and NF-κB/p65 in HSC-LX2 cells.

Group	No	p-IKB/GAPHD	p65/GAPHD
Blank control group	3	3.05254±0.1546##	3.08523±0.2166##
Negative control group	3	3.2969±0.1672	2.5584±0.1346
Model group	3	10.2218±0.6432**	8.3378±0.4321**
siRNA-Tβ4 knockdown group	3	10.8794±0.1085**	7.7758±0.1781**
Tβ4 treatment group	3	3.7448±0.2361##	3.4983±0.4925##

*p<0.05, compared with the blank control group; **p<0.01, compared with the blank control group; #p<0.05, compared with the model group; ##p<0.01, compared with the model group.

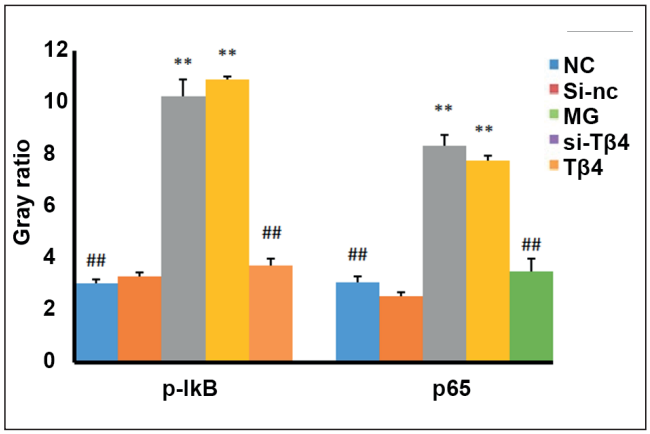

Figure 4. Tβ4-induced alteration of nucleic acid expression levels of p-IKB and NF-κB/p65 in HSC-LX2 cells (*p<0.05, compared with the blank control group; **p<0.01, compared with the blank control group; #p<0.05, compared with the model group; ##p<0.01, compared with the model group).

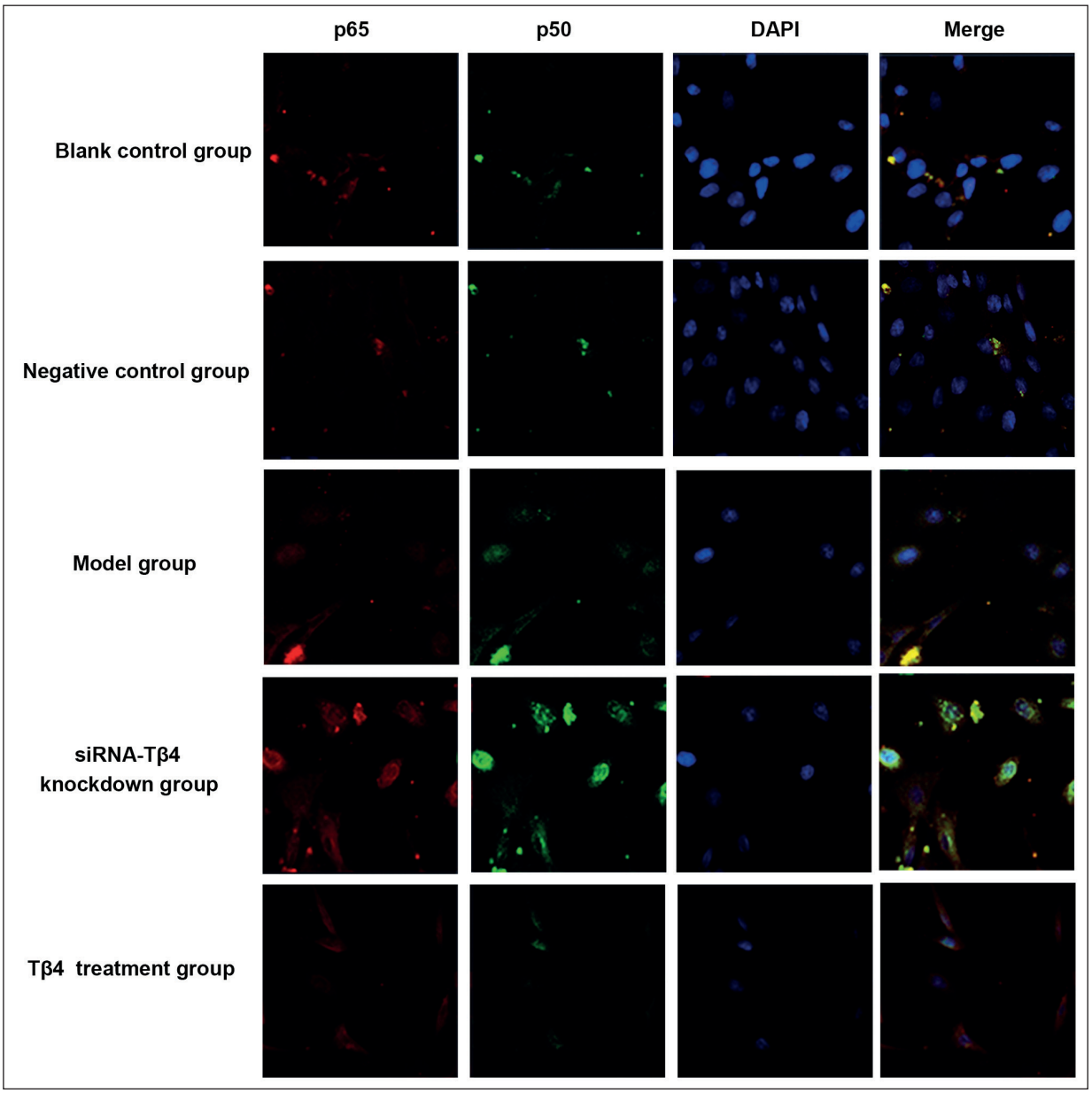

Figure 5. Tβ4 inhibition of nuclear translocation of NF-κB/p65 and NF-κB/p50 in HSC-LX2 cells.

κB/p50 and attenuated nuclear translocation. Thus, Tβ4 can inhibit nuclear translocation of NF-κB/p65 and NF-κB/p50 in HSC-LX2 cells (Figure 5).

Expression of p-IKB in HSC-LX2 Cells Detected by Immunofluorescence Staining and Laser Confocal Microscopy

There was a very low expression of cytoplasmic p-IKB in the control group, whereas in the model group and the siRNA-Tβ4 knockdown group, the fluorescence intensity increased markedly, indicating a higher expression of cytoplasmic p-IKB or higher level of IKB phosphorylation. In the Tβ4 treatment group, the fluorescence intensity decreased significantly, indicating lower level of p-IKB expression. Thus, the result suggested that Tβ4 can inhibit IKB phosphorylation in HSC-LX2 cells (see Table V and Figure 6).

Table V. Tβ4 inhibition of p-IKB expression in HSC-LX2 cells.

Group	Fluorescence intensity		
	p-IKB	p65	p50
Blank control group	0.02023±0.0208	0.00804±0.0147	0.00518±0.0042
Negative control group	0.01087±0.0021	0.00563±0.0012	0.00501±0.0063
Model group	0.08231±0.0168**	0.06671±0.0401**	0.06493±0.0269**
siRNA-Tβ4 knockdown group	0.06013±0.0247**	0.04178±0.0193**	0.04035±0.0408**
Tβ4 treatment group	0.01003±0.0235*##	0.01004±0.0054*##	0.00721±0.0041*##

*p<0.05, compared with the blank control group; **p<0.01, compared with the blank control group; #p<0.05, compared with siRNA-Tβ4 knockdown group; ##p<0.01, compared with siRNA-Tβ4 knockdown group.

Measurement of Cytoplasmic p-IKB Protein and Nuclear p65 Protein in IL-1β-Stimulated HSC-LX2 Cells After Tβ4 Treatment by Western Blot Assay

In the model group and the siRNA-Tβ4 knockdown group, the expression levels of cytoplasmic p-IKB and nuclear NF-κB/p65 were remarkably higher (p<0.01), but the levels of cytoplasmic p65 protein were markedly lower than those in the control group (p<0.05). The results suggested the occurrence of nuclear translocation of NF-κB/p65. The expression levels of cytoplasmic p-IKB and nuclear NF-κB/p65 were lower in the Tβ4 treatment group than those in the model group (p<0.01), indicating Tβ4's inhibitory effect on IKB phosphorylation in HSC-LX2 cells. Attenuated IKB phosphorylation led to less p65 protein entering into the nucleus, thereby reducing the activity of this pathway. There were no significant differences in the expression levels of these proteins between the siRNA-Tβ4 knockdown group and the model group (p>0.05, Figures 7 and 8).

Discussion

HSC proliferation and apoptosis are closely associated with the regulation of cell cycle progression[12,13]. Cell cycle regulation checkpoints are present in the G0/G1 and G2/M phases of the cell cycle, which ensure synchronous mitosis and that the downstream events are initiated when the upstream events are correctly completed in the cell cycle. Therefore, alteration of the cell cycle in the G0/G1 and G2/M phases may result in abnormal cell division, thereby affecting cell proliferation and differentiation[14]. To further investigate the cell cycle phase when apoptosis occurs, in this study, the amount of DNA in HSC-LX2 cells was detected using flow cytometry to determine the cell cycle phase. As the results showed, Tβ4 induced G0/G1 arrest in HSC-LX2 cells in the Tβ4 treatment group, preventing the cell cycle from entering the S phase normally. The number of cells in the S phase was significantly reduced, and in turn, there were less mature HSCs. The findings suggested that Tβ4 can delay cell division by arresting HSC-LX2 cells in the G0/G1 phase, thereby attenuating HSC-LX2 cell maturation and inducing apoptosis. When cells undergo apoptosis, there are changes in plasma membrane composition. For example, phosphatidylserine (PS) can be externalized. Annexin V is a Ca^{2+}-dependent phospholipid-binding protein, which can specifically bind to PS with high affinity. Apoptosis can be detected by flow cytometry using fluorescein-labeled Annexin V as a probe. As the results showed, after Tβ4 treatment, the apoptotic rate of HSC-LX2 cells was markedly higher in the Tβ4 treatment group than that in the model group (p<0.05). Phosphatidylserine externalization in membrane detected by Annexin V indicated that Tβ4 can induce apoptosis of activated hepatic stellate cells. Compared with the model group, although the apoptotic rate in the siRNA-Tβ4 knockdown group decreased, there was no statistically significant difference between the two groups (p>0.05). This indicated that siRNA-Tβ4 knockdown in HSC-LX2 cells can attenuate HSC apoptosis induced by Tβ4, thus promoting HSC activation and worsening liver fibrosis.

The NF-κB signaling pathway is a branch of the PI3K/AKT signaling pathway, and activated PI3K/AKT pathway can directly activate it, producing biological effects such as regulating cell growth and differentiation. In Tβ4 treatment of liver fibrosis, it was unknown if the NF-κB signaling pathway was involved in the regulation of HSC activation and apoptosis. Ji et al[15] reported that reversing activated HSCs to quiescence was almost impossible. Therefore, reducing the number of HSCs by apoptosis

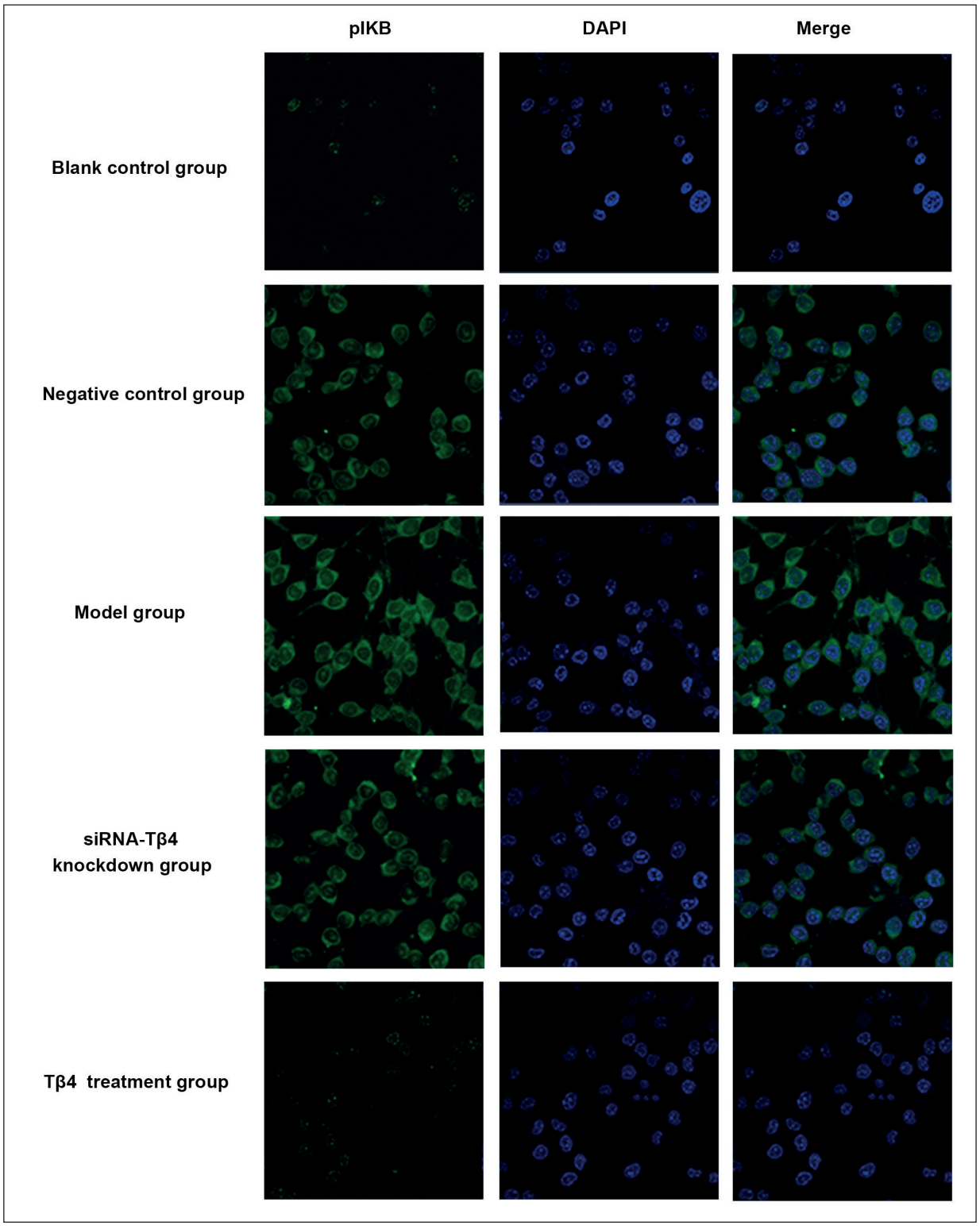

Figure 6. Tβ4 inhibition of p-IKB expression in HSC-LX2 cells.

was the main approach to reversal of liver fibrosis. The signaling pathways regulating HSC apoptosis are complicated. In recent years, activated NF-κB family-mediated apoptosis of HSCs was a hot research topic[16]. NF-κB is a nuclear protein factor that is widely present in many cells. When cells

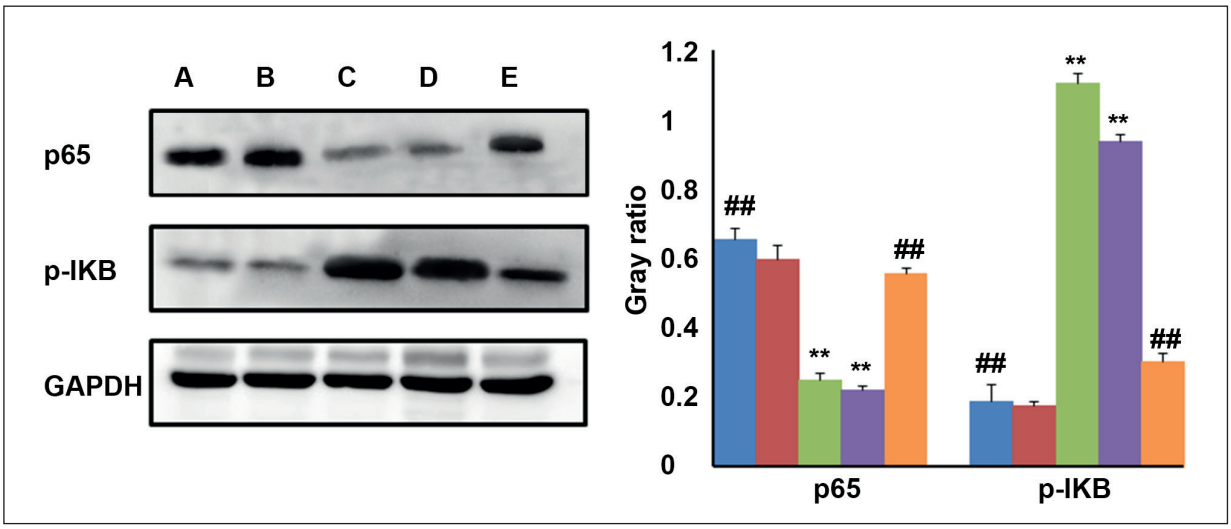

Figure 7. Expression levels of cytoplasmic p65 and p-IKB in HSC-LX2 cells after Tβ4 treatment. *p<0.05, compared with the blank control group; **p<0.01, compared with the blank control group; #p<0.05, compared with the siRNA-Tβ4 knockdown group; ##p<0.01, compared with the siRNA-Tβ4 knockdown group. **A**, blank control group. **B**, Negative control group. **C**, Model group. **D**, siRNA-Tβ4 knockdown group. **E**, Tβ4 treatment group.

are in a quiescent phase, inactivated NF-κB is present in cytosol as a heterodimer consisting of two polypeptide chains of P50 and P65. Among them, the p65 subunit binds to an inhibitory protein IκB, generating NF-kB-IκB complex as an inactivated form staying in cytoplasm[17]. All inhibitory IκB proteins contain ankyrin repeats that can mask the nuclear localization sequence of NF-kB, thereby preventing NF-kB from entering the nucleus. The NF-kB pathway is activated when cells face a crisis of survival and initiate an immune response against inflammation or invasion of bacteria, viruses or other pathogenic microorganisms. The mechanism of NF-kB activation is mainly through IκB phosphorylation, releasing NF-kB from the inactive NF-kB-IκB complex. Upon detaching from IκB, NF-κB can migrate from the cytoplasm into the nucleus. As evidence of NF-kB activation, the activated IκB protein was present in the cytoplasm in its phosphorylated form, and the p65 protein was present in the nucleus. Both proteins can be detected by Western blot.

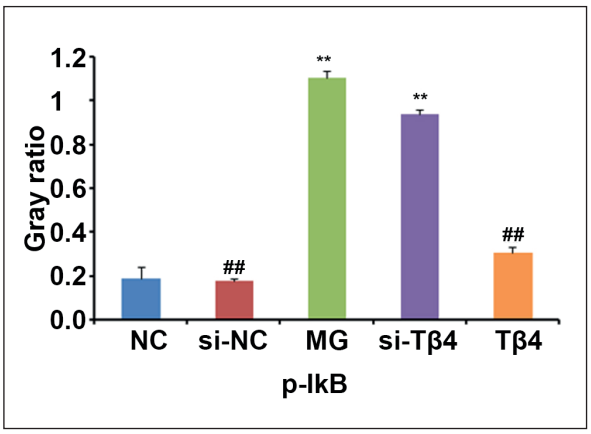

Figure 8. Expression level of nuclear NF-κB/p65 in HSC-LX2 cells after Tβ4 treatment. *p<0.05, compared with the blank control group; **p<0.01, compared with the blank control group; #p<0.05, compared with siRNA-Tβ4 knockdown group; ##p<0.01, compared with siRNA-Tβ4 knockdown group.

NF-κB is absent in the nucleus of quiescent HSCs, whereas NF-κB nuclear translocation signals were observed in activated and α-SMA positive HSCs[18]. Zheng et al[19] reported that when NF-κB nuclear translocation signals were strong, the HSC apoptotic rate was found to be increased significantly. In this work, it was found that the expression level of NF-κB/p65 was markedly increased when Tβ4 expression in HSC-LX2 cells was silenced by siRNA-Tβ4 knockdown. As the Western blot results showed, the expression levels of cytoplasmic p-IkB and nuclear NF-kB/p65 protein and mRNA were remarkably higher (p<0.05), but the expression levels of cytoplasmic NF-kB/p65 protein and mRNA were significantly lower (p<0.05) in the siRNA-Tβ4 knockdown group than in the negative control group. When fluorescence-stained cells were observed under a laser confocal microscope, it was found that the fluorescence intensity of nuclear p65 was increased in the siRNA-Tβ4 knockdown group, indicating the occurrence of

nuclear translocation. This finding suggested that Tβ4 gene knockdown in HSC-LX2 cells can markedly increase NF-kB nuclear translocation signal, resulting in the activation of the NF-kB pathway. After Tβ4 treatment, the expression levels of cytoplasmic p-IkB and nuclear NF-kB/p65 protein and mRNA in HSC-LX2 cells became significantly lower ($p<0.05$), while the levels of cytoplasmic NF-kB/p65 protein and mRNA became markedly higher ($p<0.05$) than those in the model group.

Conclusions

We showed that Tβ4 plays an important role in liver fibrosis. Loss of Tβ4 expression increases the number of activated hepatic stellate cells, leading to enhanced activity of NF-κB signaling pathway. In turn, apoptosis of HSC is attenuated and inflammatory responses are maintained. As a result, the number of HSCs is maintained at a high level, which ultimately promotes the onset and progression of liver fibrosis. Increased Tβ4 expression, on the contrary, can significantly inhibit activity of the NF-κB signaling pathway, downregulate p-IκB expression and prevent p65 from entering into the nucleus, thereby promoting apoptosis of HSCs and reversing liver fibrosis. Therefore, in the context of difficulty in evaluating efficacy and safety of anti-liver fibrosis drugs, it is of far-reaching clinical significance to carry out in-depth mechanism study of Tβ4. Whether Tβ4 can be combined with other drugs in treatment of liver fibrosis depends on clinical safety, which warrants further studies.

Conflict of Interests

The authors declare that they have no conflict of interest.

References

1) Irobi E, Aguda AH, Larsson M, Guerin C, Yin HL, Burtnick LD, Blanchoin L, Robinson RC. Structural basis of actin sequestration by thymosin-beta4: implications for WH2 proteins. EMBO J 2004; 23: 3599-3608.
2) Reyes-Gordillo K, Shah R, Popratiloff A, Fu S, Hindle A, Brody F, Rojkind M. Thymosin-beta4 (Tbeta4) blunts PDGF-dependent phosphorylation and binding of AKT to actin in hepatic stellate cells. Am J Pathol 2011; 178: 2100-2108.
3) Belsky JB, Morris DC, Bouchebl R, Filbin MR, Bobbitt KR, Jaehne AK, Rivers EP. Plasma levels of F-actin and F:G-actin ratio as potential new biomarkers in patients with septic shock. Biomarkers 2016; 21: 180-185.
4) Kim S, Kwon J. Thymosin beta4 has a major role in dermal burn wound healing that involves actin cytoskeletal remodelling via heat-shock protein 70. J Tissue Eng Regen Med 2017; 11: 1262-1273.
5) Barnaeva E, Nadezhda A, Hannappel E, Sjogren MH, Rojkind M. Thymosin beta4 upregulates the expression of hepatocyte growth factor and downregulates the expression of PDGF-beta receptor in human hepatic stellate cells. Ann N Y Acad Sci 2007; 1112: 154-160.
6) Xiao Y, Qu C, Ge W, Wang B, Wu J, Xu L, Chen Y. Depletion of thymosin beta4 promotes the proliferation, migration, and activation of human hepatic stellate cells. Cell Physiol Biochem 2014; 34: 356-367.
7) Kim J, Jung Y. Thymosin beta 4 is a potential regulator of hepatic stellate cells. Vitam Horm 2016; 102: 121-149.
8) Chen G, Wang Y, Li M, Xu T, Wang X, Hong B, Niu Y. Curcumol induces HSC-T6 cell death through suppression of Bcl-2: involvement of PI3K and NF-kappaB pathways. Eur J Pharm Sci 2014; 65: 21-28.
9) Espin-Palazon R, Traver D. The NF-kappaB family: key players during embryonic development and HSC emergence. Exp Hematol 2016; 44: 519-527.
10) Jiang M, Wu YL, Li X, Zhang Y, Xia KL, Cui BW, Lian LH, Nan JX. Oligomeric proanthocyanidin derived from grape seeds inhibited NF-kappaB signaling in activated HSC: Involvement of JNK/ERK MAPK and PI3K/Akt pathways. Biomed Pharmacother 2017; 93: 674-680.
11) Zhu L, Cheng M, Liu Y, Yao Y, Zhu Z, Zhang B, Mou Q, Cheng Y. Thymosin-beta4 inhibits proliferation and induces apoptosis of hepatic stellate cells through PI3K/AKT pathway. Oncotarget 2017; 8: 68847-68853.
12) Li Q, Li X, Deng CL. Induction of proliferation and activation of rat hepatic stellate cells via high glucose and high insulin. Eur Rev Med Pharmacol Sci 2017; 21: 5420-5429.
13) Abe T, Masuya M, Ogawa M. An efficient method for single hematopoietic stem cell engraftment in mice based on cell-cycle dormancy of hematopoietic stem cells. Exp Hematol 2010; 38: 603-608.
14) Ma HH, Yao JL, Li G, Yao CL, Chen XJ, Yang SJ. Effects of c-myb antisense RNA on TGF-beta1 and beta1-I collagen expression in cultured hepatic stellate cells. World J Gastroenterol 2004; 10: 3662-3665.
15) Ji G, Wang L, Zhang SH, Liu JW, Zheng PY, Liu T. Effect of Chinese medicine Qinggan Huoxuefang on inducing HSC apoptosis in alcoholic liver fibrosis rats. World J Gastroenterol 2006; 12: 2047-2052.
16) Fang S, Yuan J, Shi Q, Xu T, Fu Y, Wu Z, Guo W. Downregulation of UBC9 promotes apoptosis of activated human LX-2 hepatic stellate cells by

suppressing the canonical NF-kappaB signaling pathway. PLoS One 2017; 12: e0174374.

17) Wang XM, Yu DM, McCaughan GW, Gorrell MD. Fibroblast activation protein increases apoptosis, cell adhesion, and migration by the LX-2 human stellate cell line. Hepatology 2005; 42: 935-945.

18) Wang L, Yue Z, Guo M, Fang L, Bai L, Li X, Tao Y, Wang S, Liu Q, Zhi D, Zhao H. Dietary flavonoid hyperoside induces apoptosis of activated human LX-2 hepatic stellate cell by suppressing canonical NF-kappaB signaling. Biomed Res Int 2016; 2016: 1068528.

19) Zheng J, Ma LT, Ren QY, Li L, Zhang Y, Shi HJ, Liu Y, Li CH, Dou YQ, Li SD, Zhang H, Yang MH. The influence of astragalus polysaccharide and beta-elemene on LX-2 cell growth, apoptosis and activation. BMC Gastroenterol 2014; 14: 224.